Free Surface Oscillation in Sloshing Problem Predicted with ALE Method

Satoru Ushijima

Central Research Institute of Electric Power Industry (CRIEPI)
1646 Abiko, Abiko-shi, Chiba-ken, 270-1194, Japan
E-mail : ushijima@criepi.denken.or.jp

A numerical prediction method has been proposed to predict non-linear free surface oscillation in a three-dimensional container. The fluid motions are numerically predicted with Navier-Stokes equations discretized in a Lagrangian scheme with sufficient numerical accuracy. The profile of a free surface is precisely represented with three-dimensional body-fitted coordinates (BFC), which are regenerated in each computational step on the basis of the arbitrary Lagrangian-Eulerian (ALE) formulation. In order to confirm the reliability of the computational method, it was firstly applied to three-dimensional flows within complicated-shaped rigid boundaries, such as curved pipes and ducts. Then it was applied to benchmark computations related to free surface oscillations. Following these basic verifications, non-linear sloshings in a cylindrical tank and transitions from sloshing to swirling motions were numerically predicted. Throughout these computations, the applicability of the present computational method has been confirmed and some of the predicted free surface motions were visualized as sequential images and animations to understand their dynamic futures.

Key Words: non-linear sloshing, moving boundary, 3D BFC, ALE, numerical visualization

1. Introduction

The dynamic oscillation of liquid with a free surface has long been of interest in a variety of engineering fields. In particular, non-linear sloshings with large amplitudes and more complicated swirling motions are sometimes considered as the important phenomena associated with the engineering design and assessment.

In the present study, a computational technique has been proposed to predict non-linear sloshings in an arbitrarily-shaped three-dimensional container. The liquid motions are described with Navier-Stokes equations instead of velocity potential models which have been generally adopted in usual computational methods. The profile of a liquid surface is adequately represented by the three-dimensional curvilinear coordinates which are regenerated in each computational step on the basis of the arbitrary Lagrangian-Eulerian (ALE) formulation. Since the boundary conditions near the free surface can be implemented precisely in the computational space, the present method is particularly advantageous to the usual techniques in which Eulerian computational grids are adopted. Moreover, in this transformed space, the governing equations are discretized on a Lagrangian scheme in which numerical accuracy is preserved at a sufficient level.

In order to confirm the reliability of the developed computational method, it was firstly applied to the flows surrounded by complicated-shaped rigid boundaries; three dimensional flows in a curved pipe and progress of thermal stratification in a curved duct. Then, the prediction method was applied to two-dimensional free surface oscillations which have been widely taken as benchmark computations. Finally, numerical predictions were made for non-linear sloshings in a cylindrical tank and transition from sloshing to swirling motions. Some of the predicted results were numerically visualized as sequential images and animations, which allow us to understand the dynamic futures of free surface oscillations.

2. Numerical Procedure

2.1 Grid Generation

In moving boundary problems, such as free surface oscillations, it is necessary to take adequate treatment for the boundary profiles which are deformed unsteadily and non-uniformly. In the present method, non-orthogonal curvilinear coordinates, which represent the free surface profile at a given moment, are regenerated in each computational time step in order to represent its unsteady deformation.

In contrast to the Lagrangian grid generation, the ALE formulation allows us to create curvilinear coordinates independently of the liquid motion. Thus, the velocity of the computational grid point may not coincide with that of the liquid. Therefore, once a shape of the free surface is specified, the corresponding curvilinear coordinates are generated in an arbitrary-shaped three-dimensional liquid region taking this profile as one of the boundary conditions. The governing equations to generate the coordinates are given by the following Poisson equations:

$$\frac{\partial^2 \xi_m}{\partial x_i \partial x_i} = P_m \tag{1}$$

where x_i and ξ_m are coordinates in physical and transformed (or computational) spaces respectively and P_m is a control function, which is used to adjust the grid intervals in the physical space. In this paper, the Einstein summation rule is applied to the terms which have the same subscripts. To generate the coordinates, Eq.(1) is inversely transformed as

$$\left(\frac{\partial^2 x_i}{\partial \xi_p \partial \xi_q}\right)^* \left(\frac{\partial \xi_p}{\partial x_j}\right)^* \left(\frac{\partial \xi_q}{\partial x_j}\right)^* + \frac{\partial^2 x_i}{\partial \xi_r \partial \xi_s} \left(\frac{\partial \xi_r}{\partial x_j}\right)^* \left(\frac{\partial \xi_s}{\partial x_j}\right)^* + P_m \left(\frac{\partial x_i}{\partial \xi_m}\right)^* = 0 \tag{2}$$

where $p \neq q$ and $r = s$. Eq.(2) is discretized and solved with iterative computations. The terms having asterisks '*' in Eq.(2) are evaluated with cubic spline functions instead of usual central difference to increase the accuracy, as done by Ushijima [1].

In the computational space, a unit computational volume takes a simple cubic geometry and consists of 27 grid points as shown in Fig.1. The scalar variables, such as pressure,

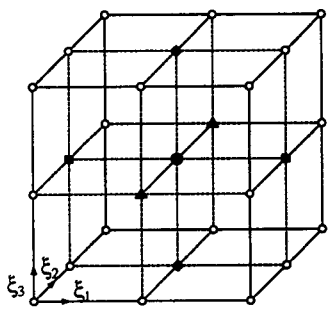

Fig. 1 Unit computational volume in transformed space

are defined at the center of the unit volume as marked by ● in Fig.1, while contravariant velocity components are placed at the center on the corresponding surface, indicated by ▲, ■ and ◆.

2.2 Governing Equations and Discretization

The incompressible liquid motion with a free surface is described by Navier-Stokes equations instead of velocity potential models, so that the three-dimensional flows can be treated more generally as rotational and viscid liquids. The governing equation is transformed into the computational space, which is given by

$$\frac{Du_i}{Dt} = -\frac{1}{\rho}\frac{\partial p}{\partial \xi_m}\frac{\partial \xi_m}{\partial x_i} + F_i + \nu\left(\frac{\partial^2 u_i}{\partial \xi_m \partial \xi_n}\frac{\partial \xi_m}{\partial x_j}\frac{\partial \xi_n}{\partial x_j} + P_m\frac{\partial u_i}{\partial \xi_m}\right) \quad (3)$$

Here u_i, F_i, p, ρ, and ν are velocity and external force in x_i direction, pressure, fluid density and kinematic viscosity, respectively. The gravity and the forced acceleration imposed to cause sloshing motions are included in F_i in Eq.(3). Since the ALE formulation is employed, the Lagrangian differential operator in Eq.(3) is given by the following form [2]:

$$\frac{D}{Dt} = \frac{\partial}{\partial \tau} + (U_m - U_{0m})\frac{\partial}{\partial \xi_m} \quad (4)$$

where t and τ are times in the physical and computational spaces respectively, which are set to be identical. The contravariant velocity components U_m and U_{0m} represent the velocity of the liquid and that of the computational grid point respectively, which are given by

$$U_m = u_i\frac{\partial \xi_m}{\partial x_i} \quad (5)$$

$$U_{0m} = \frac{\partial x_i}{\partial \tau}\frac{\partial \xi_m}{\partial x_i} \quad (6)$$

The transformed momentum equations are discretized on a Lagrangian scheme in the computational space. For convenience, Eq.(3) may be expressed in the following form:

$$\frac{Du_i}{Dt} = -PG_i + F_i + D_i \quad (7)$$

where PG_i and D_i stand for the pressure gradient and diffusion terms in Eq.(3) respectively. Equation (7) can be discretized in the following form as proposed by Ushijima [1]:

$$u_i^{n+1} = u_i'^n + \left[-PG_i^{n+1} + F_i^n + \left(\frac{3}{2}D_i'^n - \frac{1}{2}D_i''^{n-1}\right)\right]\Delta t \quad (8)$$

Here the superscript n means the computational time-step number, and prime and double prime stand for the spatial locations at the upstream points defined in the n and $n-1$ steps respectively.

2.3 LCSI for Advective Computation

The first term on the right hand side of Eq.(8), corresponding to the advection term, is calculated with local cubic spline interpolation (LCSI) method proposed by Ushijima [1].

In the one dimensional problem in ξ_m direction, for convenience, the following cubic spline function $S_m(\xi_m)$ is derived to spatially interpolate a variable ϕ at ξ_m, located between two grid points, $\xi_{m_{i-1}}$ and ξ_{m_i}:

$$S_m(\xi_m) = M_{i-1}\frac{(\xi_{m_i} - \xi_m)^3}{6h_i} + M_i\frac{(\xi_m - \xi_{m_{i-1}})^3}{6h_i} + \left(\phi_{i-1} - \frac{M_{i-1}h_i^2}{6}\right)\frac{\xi_{m_i} - \xi_m}{h_i} + \left(\phi_i - \frac{M_i h_i^2}{6}\right)\frac{\xi_m - \xi_{m_{i-1}}}{h_i} \quad (9)$$

where $h_i = \xi_{m_i} - \xi_{m_{i-1}}$. The second-order derivatives, M_{i-1} and M_i in Eq.(9), are evaluated with a third-order polynomial which is uniquely determined from the neighboring four variables located at $\xi_{m_{i-2}}$ to $\xi_{m_{i+1}}$.

In the three dimensional space, the similar spatial interpolations are repeated in all three directions, which allows us to evaluate the advection terms included in Eq.(8).

In order to confirm the accuracy of the LCSI formulation, a pure advection problem was solved with some different methods and they were compared. Fig.2 shows the scalar distributions calculated by the computational methods for advection terms. As indicated in Fig.2,

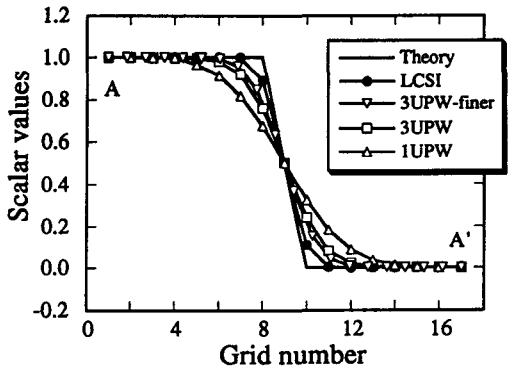

Fig. 2 Unit computational volume

it was confirmed that the present LCSI has higher accuracy than the third-order upwind difference with finer mesh division [1].

2.4 Boundary Conditions

The kinematic free surface condition is determined from the fact that the surface moves with the liquid in the physical space as

$$\frac{\partial h}{\partial t} + u_{si}\frac{\partial h}{\partial x_i} = u_{s3} \qquad [\, i = 1,2\,] \qquad (10)$$

where h is the free surface height and subscript s means that the corresponding values are defined at the grid point on the free surface.

When the viscous stresses on a liquid-gas interface are negligible, the stress conditions on free surfaces are determined by the following two equations:

$$n_i \sigma_{ij} n_j = Sk \qquad (11)$$

$$\tau_i \sigma_{ij} n_j = 0 \qquad (12)$$

where S and k mean the coefficient of surface tension and the curvature of the free surface respectively. The unit vectors n_i and τ_i are normal and tangential to the free surface and the stress tensor σ_{ij} is defined by

$$\sigma_{ij} = -p_0\delta_{ij} + \mu\left(\frac{\partial u_i}{\partial x_j} + \frac{\partial u_j}{\partial x_i}\right) \qquad (13)$$

where p_0 is the atmospheric pressure and μ means the dynamic viscosity. The detailed forms of these boundary conditions in the transformed space are indicated by Ushijima [3]. In the present paper, it is assumed that the atmospheric pressure equals zero and that the effect of surface tension can be neglected.

2.5 Solution Procedure

The main solution procedures are summarized as follows. Firstly, initial free surface profile and other necessary initial conditions are specified. Then the three-dimensional curvilinear coordinates, which are coincident with the provided free surface and the other fixed boundary shapes, are generated. In the computational space corresponding to the generated coordinates, numerical procedure for liquid calculations is performed; the convection and diffusion terms are firstly evaluated on a Lagrangian scheme and approximate velocity is derived with these values, assuming the pressure field to be given by a hydrostatic pressure distribution. After the converged correction pressure is obtained from the iterative calculations, correction velocity components and free surface levels are finally derived at a new computational step. When the unsteady numerical prediction still proceeds, the free surface profile is updated and new curvilinear coordinates are generated again for it. In this way, unsteady numerical procedure continues until the appointed time.

2.6 Numerical Visualization of Free Surface

The development of a numerical visualization technique is also important in the present study, since the predicted results are three-dimensional and they are obtained in unsteady conditions.

In the computation of sloshings, free surface profiles are represented by curvilinear coordinates regenerated in each computational step. Thus, the coordinates are saved on a hard disk at the appointed time steps during the compu-

tation. The saved data are visualized after the computation with a post processing program, which utilizes OpenGL libraries [4]. With this program, calculated results are rendered on a computer display with perspective projection and it allows us to translate and rotate the objects and also change their scales through mouse operations.

While the profile of a free surface may be drawn as a smoothly shaded model, texture mapping is much effective to make the graphics more realistic. Thus, the free surface is displayed using environment mapping, which renders an object as it were perfectly reflective; the colors on the surface are those reflected to the eye from its surroundings [4]. Some of the predicted results will be shown later with this environment mapping.

3. Application of Prediction Method

3.1 3D Flows in Curved Pipe

The developed computational method was applied to a steady flow in a pipe with a 90-degree bend, which was measured in detail with LDV by Bovendeerd et al [5].

Fig.3 shows the generated mesh for the curved pipe and Fig.4 indicates the predicted velocity vectors on the section of symmetry. The predicted axial velocity profiles in the curved area are compared with the experimental results as shown in Fig.5, where the angles of the sections are defined with respect to the entrance section of the bend. From these results, it can be seen that the predicted velocity profiles are generally in good agreement with the experimental ones.

3.2 Thermal Stratification in Curved Duct

The present computational method was also applied to the unsteady thermal stratification phenomena arising in a curved duct which has two 90-degree bends, as illustrated in Fig.6.

In experiments, a fluid with higher temperature, T_H, was initially supplied to the duct in a constant flow rate, so that the steady condition was established. After creating this steady state, the temperature of the incoming fluid was lowered from T_H to T_C during 30 seconds, where the temperature difference $T_H - T_C$ equals $10K$. The average velocity in the duct was maintained at $10mm/s$ throughout the steady and thermal transient conditions.

Fig.7 shows the distribution of the generated mesh. The unsteady computation was performed and the progress of thremal stratification was predicted as shown in Fig.8, in which visualized experimental results are indecated as well. The predicted results satisfactorily reproduce the inclined thermal interface and horizontally stratified region, which develops in the curved area on the downstream side after around 70 seconds from the thermal transient.

3.3 Free Surface Benchmark Computation

Since the reliability of the computational method has been confirmed in the fixed boundary problems as stated above, it was then applied to free surface benchmark computations.

Firstly free oscillation of a liquid surface with a small amplitude was calculated in order to confirm the conservations of mass and momentum. In the two dimensional rectangular container, which is 1.0 units in width and height as shown in Fig.9, free oscillation is caused under the gravity accelaration with a unit magnitude. The initial liquid depth is given by

$$h = 1.0 + 0.01sin[\pi(0.5 - x_1)] \qquad (14)$$

These conditions are same as adopted by Ramaswamy [6].

Fig.10 shows the time history of the free surface displacements at both sides of the container with free-slip conditions. As shown in this figure, no numerical dumpings are found and the conservations of mass and momentum are reasonably satisfied.

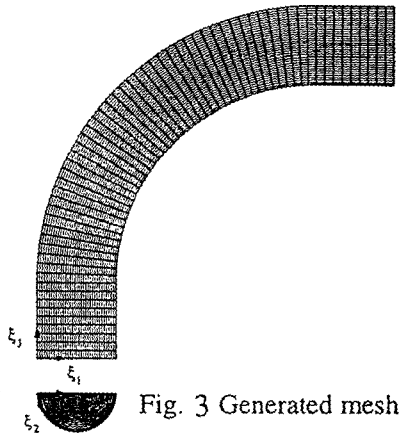

Fig. 3 Generated mesh

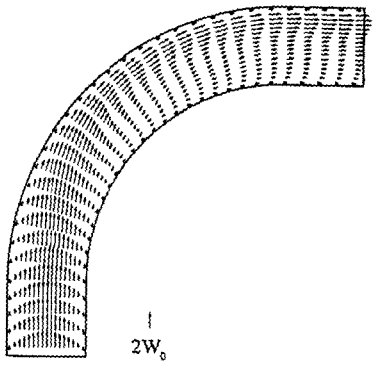

Fig. 4 Predicted velocity vectors
(W_0=average velocity)

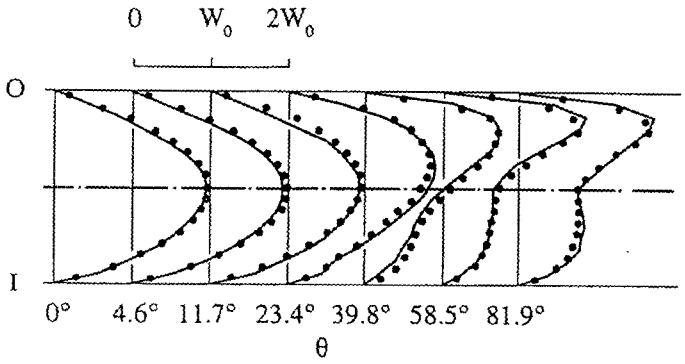

Fig. 5 Comparison of axial velocity distribution
(—experiment, ●prediction)

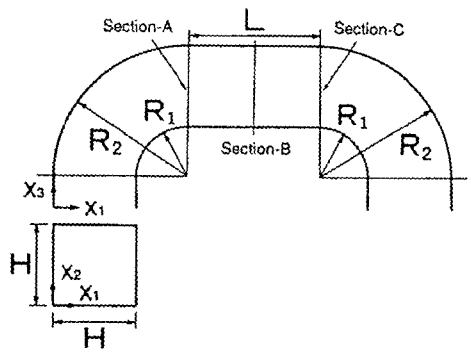

Fig. 6 Geometry of curved duct
($H = 50mm$, $L = 80mm$
$R_1 = 30mm$, $R_2 = 80mm$)

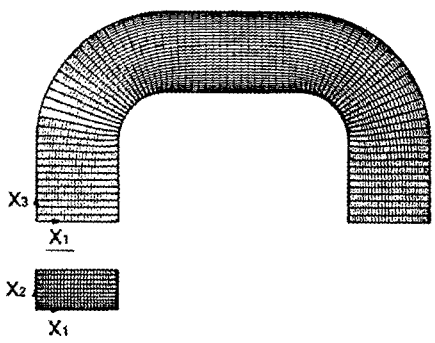

Fig. 7 Generated mesh

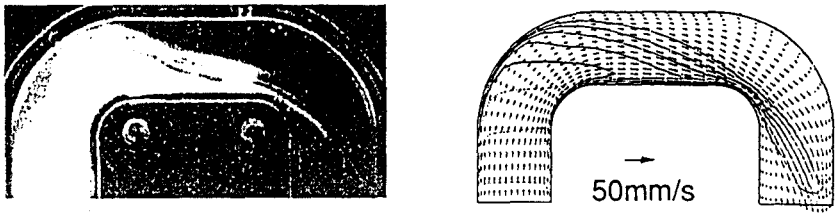

(a) t=25s

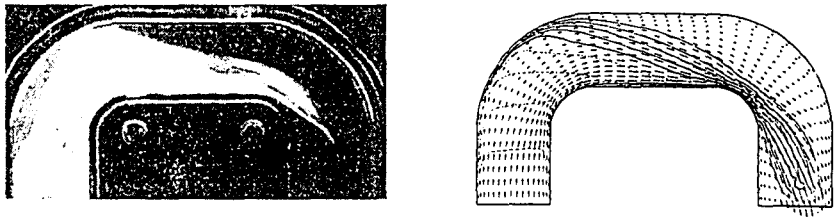

(b) t=30s

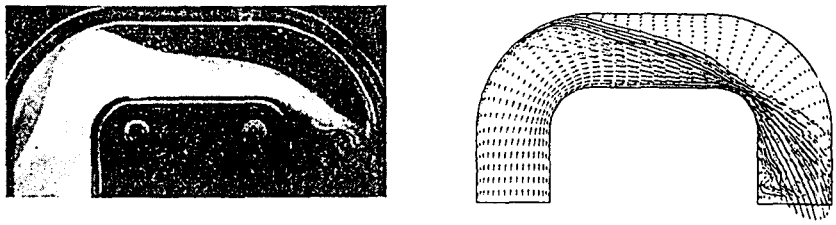

(c) t=40s

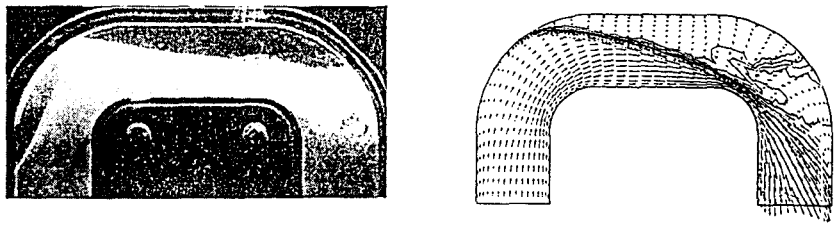

(d) t=70s

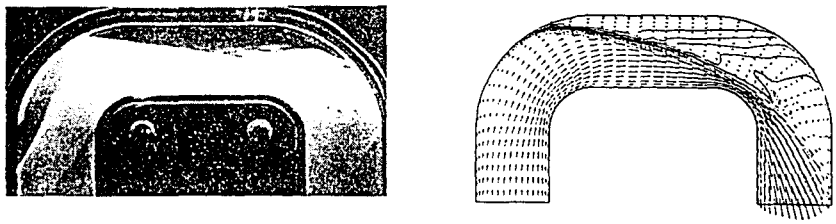

(e) t=120s

Fig. 8 Visualized thermal stratification in experiments (left) and corresponding computational results (right)

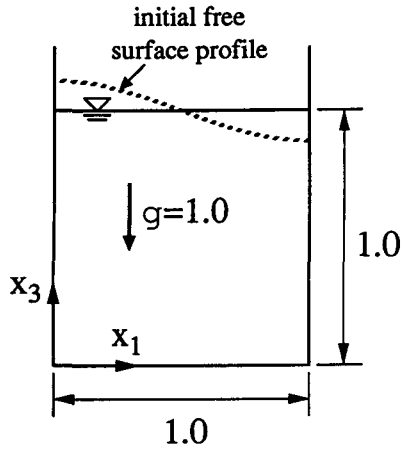

Fig. 9 Container for free oscillations

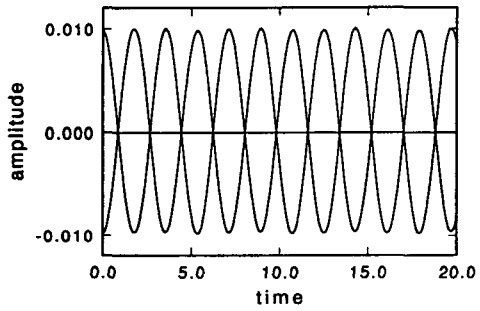

Fig. 10 free oscillation without viscous effects

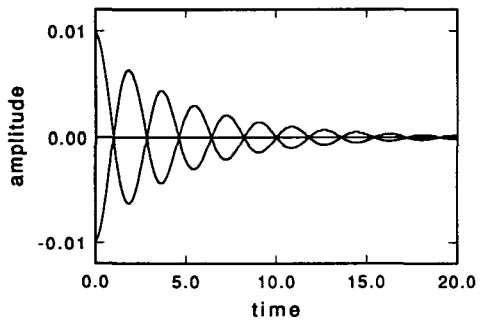

Fig. 11 free oscillation with viscous effects

On the other hand, Fig.11 shows the time history predicted with viscous conditions, in which liquid velocity is zero on the wall boundaries and kinematic viscosity of the liquid is set at 0.01. In this case, the adequate attenuation as calculated by Ramaswamy [6] is observed in the present results.

Another example is a non-linear oscillation of a free surface, which was initially investigated by Harlow and Welch [7]. This computation has also been taken as a benchmark computation by Ramaswamy [6] and many others. In this case, a liquid in a rectangular container, which is 4.8 in width and 4.0 in height as shown in Fig.12, is completely static with a horizontal free surface profile in the initial condition. The kinematic viscosity of the liquid is 0.01 and a gravity acceleration of a unit magnitude acts downwards.

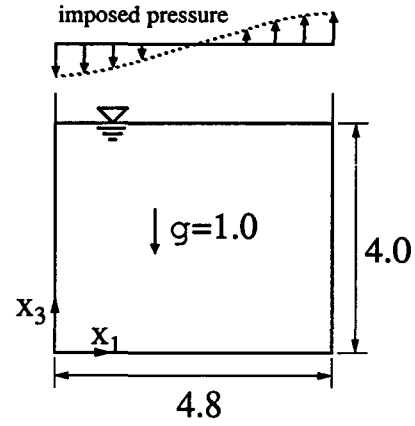

Fig. 12 Container for non-linear oscillation

At the beginning of the computation, the following cosine pressure impulse $P_0(t)$ is imposed on the free surface:

$$P_0(t) = \delta(T)\ cos(2\pi x_1/9.6) \qquad (15)$$

where $\delta(T)$ is a dirac delta function.

The time history of the free surface displacements is shown in Fig.13, in which the amplitudes of the linear analysis and the numerically predicted results by Harlow and Welch [7] are also indicated. The present computational results show the highly non-linear spike and bubble, which are quite similar to the results of Harlow and Welch [7]

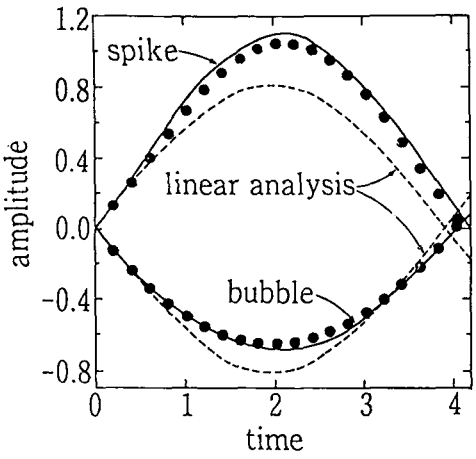

Fig. 13 Free surface displacements in nonlinear sloshing (●=preset computation, — = Harlow and Welch [7])

3.4 Sloshing in Cylindrical Tank

Following the benchmark computations, the free surface oscillations in more practical conditions were numerically predicted with the present method. Figure 14 illustrates the definition sketch, in which Cartesian coordinates and dimensions are indicated, where R and H are the radius of a cylindrical tank and the liquid depth in the static condition respectively. In a cylindrical tank with $R = H = 0.5m$,

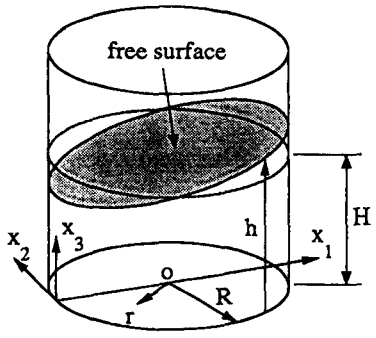

Fig. 14 Definition sketch

the liquid with the kinematic viscosity of 0.01 cm^2/s is subject to the forced acceleration in x_1 direction as given by

$$a_1(t) = -X_1\ \omega^2 \sin(\omega t) \qquad (16)$$

where the amplitude X_1 and angular frequency ω of the forced displacement in x_1 direction are $2mm$ and $10.22\ radian/sec$, respectively. This external vibration coincides with the (1,2) mode of the natural frequency [8]. Figure 15 shows a series of the predicted free surface profiles, which are visualized with the environment mapping described in the section 2.6, together with the bottom and side boundaries displayed as wire-frame surfaces.

3.5 Swirling Motion of Free Surface

It has been reported that when an axisymmetrical tank of liquid is subject to a harmonic vibration in a single horizontal direction, the free surface motion may rotate harmonically or non-harmonically around the vertical axis of the tank. This swirling motion of waves was observed by Hutton [9] in a cylindrical tank laterally oscillated at the frequencies just below the lowest natural frequency. In the present investigation, transition from non-linear sloshing to swirling motions in a cylindrical tank is numerically predicted by setting up the same initial trigger in x_2-direction, as employed by Tanaka and Nakayama [10]:

$$a_2(t) = \begin{cases} X_2 \sin(2\pi f t) & [\ 0 \le t \le 3\ (s)\ ] \\ 0 & [\ 3\ (s) < t\ ] \end{cases} \qquad (17)$$

In addition, the following harmonic vibration is continuously imposed in x_1-direction:

$$a_1(t) = X_1 \sin(2\pi f t) \qquad [\ 0 \le t\ ] \qquad (18)$$

where $X_1 = -0.0178g$ and $X_2 = X_1 \sin(\pi t/6)$. The geometries of the cylindrical tank are $R = 0.5m$ and $H = 0.6m$. While the natural frequency of (1,1) mode equals 0.944 Hz in the present geometries, the calculation is performed by setting $f = 0.940Hz$, as done by Tanaka and Nakayama [10].

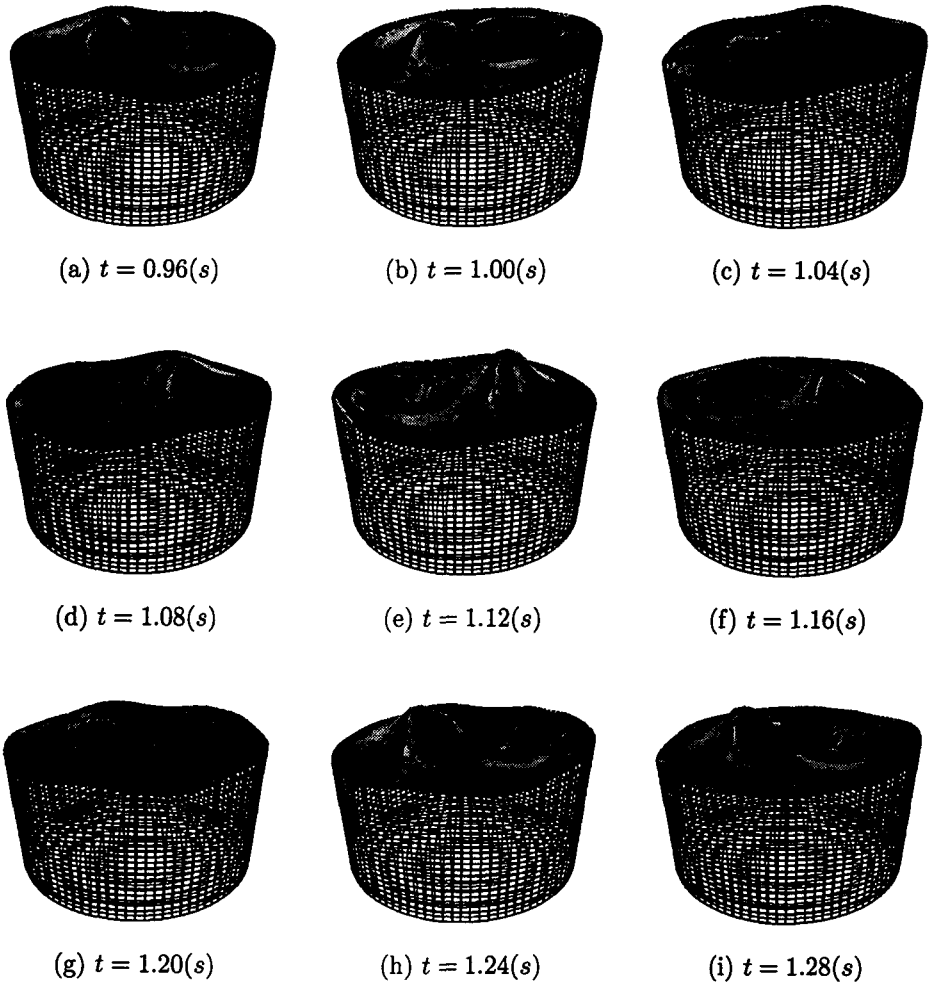

(a) $t = 0.96(s)$ (b) $t = 1.00(s)$ (c) $t = 1.04(s)$

(d) $t = 1.08(s)$ (e) $t = 1.12(s)$ (f) $t = 1.16(s)$

(g) $t = 1.20(s)$ (h) $t = 1.24(s)$ (i) $t = 1.28(s)$

Fig. 15 Visualized (1,2) mode sloshing

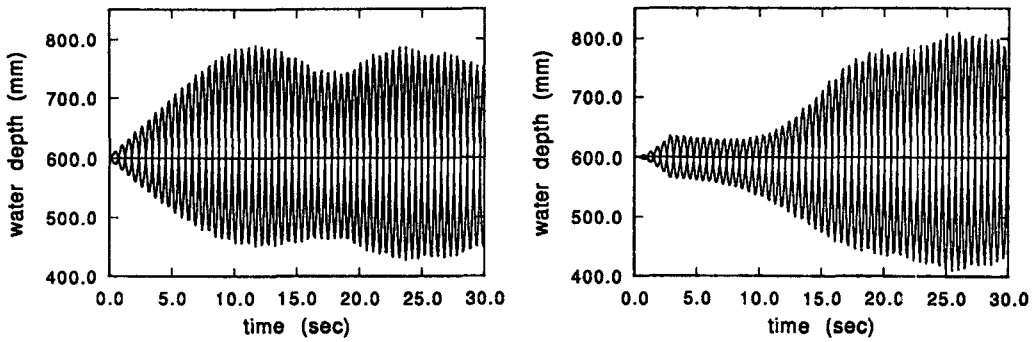

(a) $(x_1, x_2) = (0, 0)$ and $(2R, 0)$ (b) $(x_1, x_2) = (R, -R)$ and (R, R)

Fig. 16 Time history of free surface displacement at $f = 0.940\ Hz$

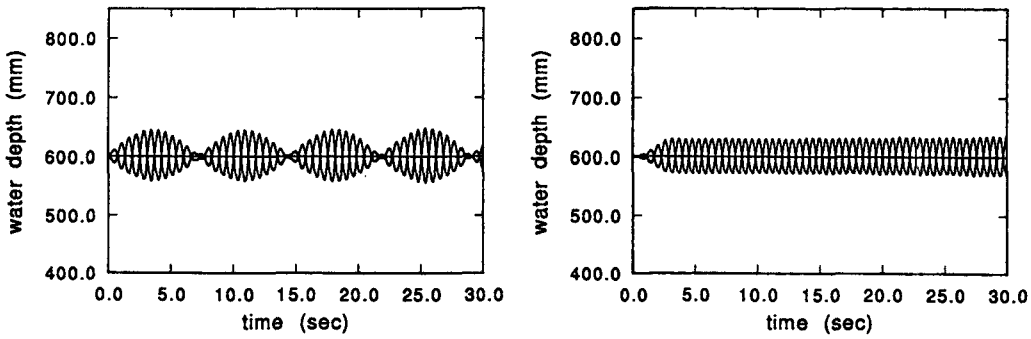

(a) $(x_1, x_2) = (0, 0)$ and $(2R, 0)$ (b) $(x_1, x_2) = (R, -R)$ and (R, R)

Fig. 17 Time history of free surface displacement at $f = 0.796\ Hz$

Figure 16 (a) and (b) show the surface displacements at $(x_1, x_2) = (0, 0)$ and $(2R, 0)$, and $(x_1, x_2) = (R, -R)$ and (R, R), respectively. On the plane of principal excitation, $x_1 - x_3$ plane, a large non-linear response gradually develops, as shown in Fig.16 (a). On the other hand, while relatively small oscillation continues on $x_2 - x_3$ plane in the initial stage, as shown in Fig.16 (b), the amplitudes becomes larger at around $t = 10s$, which indicates the transition to swirling motion of the free surface. In contrast, when the frequency of principal force is set at $f = 0.796Hz$, no transition to swirling motions appears as shown in Fig.17.

4. Concluding Remarks

A numerical prediction method has been proposed to predict non-linear free surface oscillation in a three-dimensional container. In the present method, the fluid motions are numerically predicted with Navier-Stokes equations and the profile of a free surface is precisely represented with 3D BFC, which are regenerated in every computational step on the basis of an ALE method.

In order to confirm the accuracy of the developed computational method, it was firstly applied to three dimensional flows in a curved pipe and thermally stratified flows in a curved duct. Then it was applied to two-dimensional free surface oscillations which have been widely taken as benchmark computations. Finally, following these verifications, non-linear sloshings in a cylindrical tank and transitions from sloshing to swirling motions were numerically predicted. Throughout these computations, it can be seen that the present computational method has reasonable applicability to various free surface oscillations.

References

[1] S. Ushijima. Prediction of thermal stratification in a curved duct with 3D boundary-fitted co-ordinates. *International Journal for Numerical Methods in Fluids*, 19:647–665, 1994.

[2] S. Ushijima. Arbitrary Lagrangian-Eulerian numerical prediction for local scour caused by turbulent flows. *Journal of Computational Physics*, 125:71–82, 1996.

[3] S. Ushijima. Three-dimensional arbitrary Lagrangian-Eulerian numerical prediction method for non-linear free surface oscillation. *International Journal for Numerical Methods in Fluids*, 26:605–623, 1998.

[4] J. Neider, T. Davis and M. Woo. *OpenGL Programming Guide.* Addison-Wesley Publishing Company, 1993.

[5] F. N. Van de Vosse P. H. M. Bovendeerd, A. A. Van Steenhoven and G. Vossers. Steady entry flow in a curved pile. *J. Fluid Mech.*, 177:233–246, 1987.

[6] B. Ramaswamy. Numerical simulation of unsteady viscous free surface flow. *Journal of Computational Physics*, 90:396–430, 1990.

[7] F. H. Harlow and J. E. Welch. Numerical calculation of time-dependent viscous incompressible flow of fluid with free surface. *Phys. Fluids*, 8(12):2182–2189, 1965.

[8] H. Lamb. *Hydrodynamics.* Cambridge University Press., 6th edition edition, 1932.

[9] R. E. Hutton. An investigation of resonant, nonlinear, nonplanar free surface oscillations of a fluid. *NASA Technical Note*, D-1870, 1963.

[10] H. Tanaka and T. Nakayama. A boundary element method for the analysis of nonlinear sloshing in three-dimensional containers (in Japanese). *Trans. JSME*, 57(538):1934–1940, 1991.